a value for the valence band to Γ_{15} gap of the order of 2 eV, this would certainly improve our agreement for the Faraday effect, although it would raise some theoretical questions.

ACKNOWLEDGMENTS

The author has benefited from discussions of this work with Dr. B. Lax, Dr. H. Bennett, and Dr. H. J. Zeiger.

PHYSICAL REVIEW VOLUME 133, NUMBER 2A 20 JANUARY 1964

Spontaneous and Stimulated Recombination Radiation in Semiconductors*

GORDON LASHER† AND FRANK STERN
IBM Watson Research Center, Yorktown Heights, New York
(Received 17 July 1963; revised manuscript received 13 September 1963)

Spectral line shapes of the radiation produced by band-to-band recombination of excess carriers in semiconductors are calculated under the assumption that the momentum matrix element is the same for all initial and final states, i.e., that there is no momentum selection rule. The peak of the stimulated radiation falls at a lower photon energy than does the peak of the spontaneous radiation, except when $T=0°K$. Some numerical results are given for simple parabolic bands, specifically for the case of electron injection into p-type GaAs, and are used to deduce the temperature dependence of the forward current which is necessary to maintain a fixed gain in the active region of a diode. The result is closely related to the temperature dependence of the threshold current in an injection laser, and gives reasonable agreement with experiment. The effect of a conduction band tail is briefly considered.

I. INTRODUCTION

RADIATIVE recombination is one of the principal processes by which electrons and holes present in excess of the thermal equilibrium concentrations can recombine in semiconductors, and has been extensively studied.[1–8] In most cases considered heretofore the radiative recombination has been primarily spontaneous radiation. However, the discovery of injection lasers[9–11] has confirmed the conjecture that photon populations can be high enough to give a substantial amount of stimulated emission.[12,13] In this paper, we calculate, on the basis of a simple model, the spectral line shape of the spontaneous and stimulated radiation emitted in band-to-band recombination. The actual line shape of the radiation emitted depends on the boundary conditions and the operating conditions of a particular experiment, and is illustrated by a number of examples.

We restrict our attention to the case of band-to-band transitions, because we believe this case to be the best approximation in semiconductors in which substantial concentrations of shallow impurities are present, causing the impurity levels to merge with adjacent bands. Other models can, of course, be more applicable in other cases. For example, transitions between states of isolated impurities are responsible for the red emission of the ruby laser, and such systems have been studied in considerable detail.[14] Transitions between a band and one or more impurity levels may also be important, and results for this case have been obtained by Eagles[15] and by Dumke.[16]

In the next section we give some general results concerning the spontaneous and stimulated spectral functions, and in Sec. III we give more specific results for the case of transitions with no selection rule between simple parabolic conduction and valence bands with

* A brief account of this work was presented at the American Physical Society Meeting in St. Louis, Missouri, in March, 1963 [Bull. Am. Phys. Soc. 8, 201 (1963)].

† The work of this author was supported in part by the U. S. Army Electronics Research & Development Laboratory under contract No. DA 36-029 SC-90711.

[1] J. R. Haynes, M. Lax, and W. F. Flood, Phys. Chem. Solids 8, 392 (1959), (Ge, Si).

[2] R. Braunstein, Phys. Rev. **99**, 1892 (1955), (GaSb, GaAs).

[3] M. I. Nathan and G. Burns, Phys. Rev. **129**, 125 (1963), (GaAs).

[4] R. J. Keyes and T. M. Quist, Proc. IRE **50**, 1822 (1962), (GaAs).

[5] H. G. Grimmeiss and H. Koelmans, Phys. Rev. **123**, 1939 (1961), (GaP).

[6] M. Gershenzon and R. M. Mikulyak, Solid-State Electron. **5**, 313 (1962), (GaP).

[7] H. G. Grimmeiss and H. Koelmans, Z. Naturforsch. **14a**, 264 (1959), (GaN).

[8] C. Benoit à la Guillaume and P. Lavallard, *Report of the International Conference on The Physics of Semiconductors, Exeter, 1962* (The Institute of Physics and The Physical Society, London, 1962), p. 875 (InSb).

[9] R. N. Hall, G. E. Fenner, J. D. Kingsley, T. J. Soltys, and R. O. Carlson, Phys. Rev. Letters **9**, 366 (1962).

[10] M. I. Nathan, W. P. Dumke, G. Burns, F. H. Dill, Jr., and G. J. Lasher, Appl. Phys. Letters **1**, 62 (1962).

[11] T. M. Quist, R. H. Rediker, R. J. Keyes, W. E. Krag, B. Lax, A. L. McWhorter, and H. J. Zeiger, Appl. Phys. Letters **1**, 91 (1962); I. Melngailis, Appl. Phys. Letters **2**, 176 (1963); K. Weiser and R. S. Levitt, Appl. Phys. Letters **2**, 178 (1963); V. S. Bagaev, N. G. Basov, B. M. Vul, B. D. Kopylovskii, O. N. Krokhin, E. P. Markin, Yu. M. Popov, A. N. Khvoshcev, and A. P. Shotov, Doklady Akad. Nauk. SSSR **150**, 275 (1963).

[12] W. P. Dumke, Phys. Rev. **127**, 1559 (1962).

[13] W. P. Dumke, IBM J. Res. Develop. **7**, 66 (1963).

[14] See, for example, B. L. Lengyel, *Lasers* (John Wiley & Sons, Inc., New York, 1962).

[15] D. M. Eagles, Phys. Chem. Solids **16**, 76 (1960).

[16] W. P. Dumke, in *Proceedings of The Symposium on Optical Masers, Brooklyn Polytechnic Institute, 1963* (to be published), and private communications.

particular reference to gallium arsenide in Sec. IV. The over-all line shape to be expected in actual structures is discussed briefly in Sec. V. In Sec. VI we give results for the temperature dependence of the threshold current for GaAs diodes which are in good agreement with experiment. Other authors have calculated threshold currents which vary as $T^{3/2}$.[17] In the last section, we briefly consider the effect of a tail in the density of states on the spontaneous line shape.

II. GENERAL CONSIDERATIONS

In an optically isotropic medium we can write for the rate at which photons are emitted per unit volume into solid angle $d\Omega$ and energy interval dE,[18]

$$r(E)dE(d\Omega/4\pi)=[r_{\text{spon}}(E)+\mathfrak{N}r_{\text{stim}}(E)]dE(d\Omega/4\pi)\,, \quad (1)$$

where $\mathfrak{N}$ is the number of photons per mode, given for thermal equilibrium by

$$\mathfrak{N}_0(E)=[\exp(E/KT)-1]^{-1}; \quad (2)$$

K is Boltzmann's constant, and T is the absolute temperature. The term $r_{\text{spon}}(E)$ in Eq. (1) gives the rate of spontaneous downward transitions of the electronic system, and $\mathfrak{N}r_{\text{stim}}(E)$ is the difference between the stimulated rates of downward and upward transitions. For band-to-band transitions the spontaneous and stimulated emission functions can be written,[19]

$$r_{\text{spon}}(E)dE=\sum(4Ne^2E/m^2\hbar^2c^3)|\mathfrak{M}|^2f_u(1-f_l)\,, \quad (3a)$$

$$r_{\text{stim}}(E)dE=\sum(4Ne^2E/m^2\hbar^2c^3)|\mathfrak{M}|^2(f_u-f_l)\,, \quad (3b)$$

where f_u and f_l are the probabilities that the upper and lower states involved in the transition are occupied, N is the index of refraction, and the sum is taken over all pairs of states per unit volume whose energy difference is between E and $E+dE$. The matrix element is averaged over all polarizations of the incident light so that

$$|\mathfrak{M}|^2=\tfrac{1}{3}\{|\mathfrak{M}_x|^2+|\mathfrak{M}_y|^2+|\mathfrak{M}_z|^2\}\,, \quad (4a)$$

$$\mathfrak{M}_x=-i\hbar(\psi_u|\exp(i\mathbf{k}\cdot\mathbf{r})(\partial/\partial x)|\psi_l)\,, \quad (4b)$$

where ψ_u and ψ_l are the wave functions of the upper and lower states, and $\mathbf{k}$ is the propagation vector of the radiation.

If the wave functions of the upper and lower states are Bloch functions characterized by wave vectors $\mathbf{k}_u$ and $\mathbf{k}_l$, respectively, then the matrix element will contain a delta function $\delta(\mathbf{k}_u-\mathbf{k}_l\pm\mathbf{k})$ to express the conservation of momentum. We can usually neglect $\mathbf{k}$ compared to $\mathbf{k}_u$ and $\mathbf{k}_l$, and set $\mathbf{k}_u=\mathbf{k}_l$. Then, if the energies E_u and E_l of the upper and lower bands are monotonic functions of $k_b=|\mathbf{k}_u|=|\mathbf{k}_l|$, the values of E_u and E_l, and the corresponding occupation probabilities f_u and f_l, are uniquely determined by the photon energy E of the incident light, and we can write

$$r_{\text{spon}}(E)=(4Ne^2E/m^2\hbar^2c^3)|\mathfrak{M}|^2\rho_{\text{red}}(E)f_u(1-f_l)\,, \quad (5a)$$

$$r_{\text{stim}}(E)=(4Ne^2E/m^2\hbar^2c^3)|\mathfrak{M}|^2\rho_{\text{red}}(E)(f_u-f_l)\,, \quad (5b)$$

where $\rho_{\text{red}}(E)$ is a reduced density of states for one direction of spin:

$$\rho_{\text{red}}(E)=(2\pi^2)^{-1}k_b^2[d(E_u-E_l)/dk_b]\,, \quad (5c)$$

and the derivative is evaluated for $E_u-E_l=E$. If several valence bands enter, we sum expressions like (5a) and (5b) over these bands. We must also sum over spins, taking the spin conservation in the matrix element into account.

We can deduce expressions for the total spontaneous recombination rate $\mathcal{R}_{\text{spon}}=\int r_{\text{spon}}(E)dE$ from (5a) in two simple limiting cases. The first is that the valence band is degenerate, so that we can take $f_l=0$ for all the transitions of interest. In that case, if we assume that the conduction band effective mass is m_c, and that the valence band has degenerate light and heavy-hole bands, with heavy-hole effective mass m_{vh} and light-hole effective mass m_{vl}, we find that

$$\mathcal{R}_{\text{spon}}=(8Ne^2E/m^2\hbar^2c^3)\langle|\mathfrak{M}_b|^2\rangle_{\text{av}}\times\{[1+(m_c/m_{vh})]^{-3/2}+[1+(m_c/m_{vl})]^{-3/2}\}n\,, \quad (5d)$$

where n is the electron concentration, and $\langle|\mathfrak{M}_b|^2\rangle_{\text{av}}$ is the average matrix element connecting states near the band edges.

The other simple result for $\mathcal{R}_{\text{spon}}$ obtains if both the conduction and valence band populations are nondegenerate. In that case we find

$$\mathcal{R}_{\text{spon}}=\frac{4Ne^2E}{m^2\hbar^2c^3}\left(\frac{2\pi\hbar^2}{mKT}\right)^{3/2}\langle|\mathfrak{M}_b|^2\rangle_{\text{av}}\times\frac{[m_{vl}/(m_c+m_{vl})]^{3/2}+[m_{vh}/(m_c+m_{vh})]^{3/2}}{(m_{vl}/m)^{3/2}+(m_{vh}/m)^{3/2}}np\,, \quad (5e)$$

where p is the hole concentration.

At the opposite extreme to the case of a direct transition selection rule, given in (5), is the case in which the matrix element is the same for all initial and final states. In that case, the more general expressions in (3) again simplify, and we can write

$$r_{\text{spon}}(E)=B\int\rho_c(E')\rho_v(E'-E)\times f_u(E')[1-f_l(E'-E)]dE'\,, \quad (6a)$$

$$r_{\text{stim}}(E)=B\int\rho_c(E')\rho_v(E'-E)\times[f_u(E')-f_l(E'-E)]dE'\,, \quad (6b)$$

[17] J. L. Moll and J. F. Gibbons, IBM J. Res. Develop. 7, 157 (1963); S. Mayburg, J. Appl. Phys. 34, 1791 (1963).

[18] See, for example, F. Stern, in *Solid State Physics*, edited by F. Seitz and D. Turnbull (Academic Press Inc., New York, 1963), Vol. 15, Sec. 36.

[19] This equation is a slightly generalized form of Eq. (36.8) in Ref. 18. We assume the material to be nonmagnetic in the present work.

where ρ_c and ρ_v are the densities of states for both spin directions per unit volume and unit energy in the conduction band and in the valence band or bands. The coefficient B is given by

$$B=(4Ne^2E/m^2\hbar^2c^3)\langle|\mathfrak{M}|^2\rangle_{\text{av}}V\,, \tag{6c}$$

where $\langle|\mathfrak{M}|^2\rangle_{\text{av}}$ is the average of the squared matrix element over spins in the upper and lower bands, and V is the volume of the crystal, which will drop out when the explicit result for $\langle|\mathfrak{M}|^2\rangle_{\text{av}}$ is used [see Eq. (12)]. The total emission rate is particularly simple when there is no selection rule, since one can integrate over conduction and valence bands independently to find

$$\mathcal{R}_{\text{spon}}=Bnp\,, \tag{6d}$$

where n and p are the concentrations of electrons and holes. $\mathcal{R}_{\text{spon}}$ gives the rate at which photons are spontaneously emitted in unit volume; thus the coefficient B has dimensions cm^3/sec.

If we assume that the electrons in the upper band are in equilibrium with each other, and characterized by quasi-Fermi level F_n, and that the holes in the lower band or bands are in equilibrium with each other and characterized by a quasi-Fermi level F_p, then we can write

$$f_u=\{1+\exp[(E_u-F_n)/KT]\}^{-1}\,, \tag{7a}$$

$$f_l=\{1+\exp[(E_l-F_p)/KT]\}^{-1}\,. \tag{7b}$$

From these relations we find that, no matter what we assume about the matrix elements which enter in (3a) and (3b), the stimulated and spontaneous functions are related to each other by[20,21]

$$r_{\text{stim}}(E)=r_{\text{spon}}(E)\{1-\exp[(E-\Delta F)/KT]\}\,, \tag{8}$$

where $\Delta F=F_n-F_p$ is the difference of the quasi-Fermi levels, and vanishes in thermal equilibrium. Thus, we find from Eqs. (1), (2), and (8) that in thermal equilibrium the spontaneous emission in each energy interval equals in magnitude the absorption stimulated by blackbody radiation, as it should.

The stimulated function r_{stim} is related to the absorption coefficient $\alpha(E)$ by[18]

$$\alpha(E)=-(\pi^2c^2\hbar^3/N^2E^2)r_{\text{stim}}(E)\,, \tag{9}$$

where the minus sign arises because we have defined $r_{\text{stim}}(E)$ to be positive when radiation is emitted, while the absorption coefficient is positive when radiation is absorbed. We can combine (8) and (9) to find

$$r_{\text{spon}}(E)=(N^2E^2/\pi^2c^2\hbar^3)\alpha(E)\times\{\exp[(E-\Delta F)/KT]-1\}^{-1}\,. \tag{10}$$

[20] The derivation of Eq. (8) is based on the occupation probabilities for independent levels, given in Eq. (7). A derivation of this result for a simple case involving impurity levels is given in the Appendix.

[21] We implicitly assume that the only interaction of the electronic system is with radiation. If interactions with lattice vibrations are important, the relation between the spontaneous and stimulated rates may be appreciably altered. See W. B. Fowler and D. L. Dexter, Phys. Rev. **128**, 2154 (1962).

If the total spontaneous emission rate is given by $\mathcal{R}_{\text{spon}}=Bnp$, and the np product is known for thermal equilibrium, we can use Eq. (10) to deduce the value of B from the optical absorption coefficient.[22] If the system is excited (in the absence of trapping) to give electron and hole populations $n_0+\Delta n$ and $p_0+\Delta n$, where n_0 and p_0 are the values for thermal equilibrium, the net rate of radiative decay toward the equilibrium carrier concentrations is $\mathcal{R}_{\text{net}}=B[(n_0+\Delta n)(p_0+\Delta n)-n_0p_0]$, and the radiative recombination lifetime when $\Delta n\ll n_0+p_0$ is

$$\tau_{\text{rad}}=\Delta n/\mathcal{R}_{\text{net}}=[B(n_0+p_0)]^{-1}\,. \tag{11}$$

This method of deducing the radiative lifetime may fail if the system is far from equilibrium, since the optical absorption will begin to deviate from its thermal equilibrium value.

The method of Van Roosbroeck and Shockley[22] is applicable to a material in which there is no **k**-selection rule, or to a nondegenerate material in which there is a selection rule, since both of these, as shown in Eqs. (5e) and (6d), have $\mathcal{R}_{\text{spon}}=Bnp$. On the other hand, if Eq. (5d) applies, the radiative lifetime of excess electrons is $n/\mathcal{R}_{\text{spon}}$, which is the shortest radiative electron lifetime possible under any assumptions about the selection rules.[23]

III. APPLICATION TO THE CASE OF PARABOLIC BANDS, NO k-SELECTION RULE

The conventional theory of direct optical absorption in crystals allows transitions only between electronic states of the same wave vector, **k**, since the momentum of a photon can be neglected on the scale of the Brillouin zone. When impurities or defects are present the wave functions and matrix elements will be modified. For low-impurity concentrations, the wave function of the lowest bound state associated with a shallow impurity level is a superpositions of wave functions of states near the adjacent band edge. The average matrix element between this state and a state across the energy gap whose wave vector has magnitude k_b is given, on the hydrogenic model, by[15]

$$\langle|\mathfrak{M}|^2\rangle_{\text{av}}=64\pi a^{*3}(1+a^{*2}k_b^2)^{-4}V^{-1}\langle|\mathfrak{M}_b|^2\rangle_{\text{av}}\,, \tag{12}$$

where $a^*=(\kappa m/m^*)a_0$ is the effective Bohr radius, m^* is the effective mass of the band edge perturbed by the impurity, κ is the static dielectric constant of the material, $a_0=\hbar^2/me^2$ is the Bohr radius, and $\langle|\mathfrak{M}_b|^2\rangle_{\text{av}}$ is the average matrix element joining states at the conduction and valence band edges in pure material. An equation similar to (12) can also be written for the excited states of the impurity. The wave functions in the continuum will also be affected, so that the k-

[22] W. van Roosbroeck and W. Shockley, Phys. Rev. **94**, 1558 (1954).

[23] W. P. Dumke, Phys. Rev. **132**, 1998 (1963).

selection rule will not apply even for these states when impurities are present.

When the impurity density becomes sufficiently large, the impurity levels broaden and merge with the adjacent band edges. The effect of such high impurity concentrations can be approximated by a rigid shift toward the center of the gap with some change in effective mass,[24] and by a tail extending into the forbidden gap which arises from the random impurity distribution.[25]

States far in the tail arise from interactions with two or more impurity ions in a cluster. They will have appreciable matrix elements with states in the opposite band over a wider range of values of k_b than does a simple hydrogenic level whose matrix element is given by (12).[26] As one goes away from the gap and into the band, the perturbation of the wave functions by the impurities decreases, and eventually a **k**-selection rule will again be approximately fulfilled.

Thus, the matrix element between conduction band and valence band states when impurity levels have merged with one or both band edges will be a complicated function of energy. Even the density of states for this problem has not been calculated in complete detail, while we must know the wave functions to calculate the matrix element. It is clear that the **k**-selection rule will not be valid near the absorption edge. We go to the opposite extreme and assume that the matrix element is constant for those transitions involved in radiative recombination, and take for the value of the matrix element the value for isolated impurities given by Eq. (12) for the limit of small k_b. The assumption is crude, but we shall show that it leads to results in fair agreement with experiment.

For transitions involving the conduction and valence band edges at $\mathbf{k}=0$ in III–V intermetallic semiconductors, we find, on averaging over polarizations of the light, and noting that spin is unchanged in a dipole transition, that

$$\langle|\mathfrak{M}_b|^2\rangle_{\text{av}}=m^2P^2/6\hbar^2\approx(m^2E_g/12m_c)\times[(E_g+\Delta)/(E_g+\tfrac{2}{3}\Delta)], \quad (13)$$

where P is the interband matrix element introduced by Kane.[27] The second equality in (13), in which Δ is the spin-orbit splitting and E_g is the energy gap, holds approximately if the interaction between conduction and valence bands dominates all other contributions to the conduction band effective mass m_c.

We can combine these results to obtain expressions for the spontaneous and stimulated functions in which the effective masses and other material parameters appear only in the multiplying factor, and in which the only essential parameters are the temperature and the quasi-Fermi levels. The result is

$$C^{-1}r_{\text{spon}}(E)=\int_0^{E-E_g}E'^{1/2}(E-E_g-E')^{1/2}f_u(1-f_l)dE', \quad (14a)$$

$$C^{-1}r_{\text{stim}}(E)=\int_0^{E-E_g}E'^{1/2}(E-E_g-E')^{1/2}(f_u-f_l)dE', \quad (14b)$$

where

$$f_u=\{1+\exp[(E'-F'_n)/KT]\}^{-1}, \quad (14c)$$

$$f_l=\{1+\exp[(E'+E_g+F'_p-E)/KT]\}^{-1}; \quad (14d)$$

we introduced $F'_n=F_n-E_c$ and $F'_p=E_v-F_p$ to represent the quasi-Fermi levels of electrons and holes with respect to the band edges at E_c and E_v. From (6) and (13) we have

$$C=(128/3\pi^3\hbar^2me^4c^3)\frac{m_c^{1/2}m_v^{3/2}m}{m^{*3}}\frac{E_g+\Delta}{E_g+\frac{2}{3}\Delta}NEE_g\kappa^3,$$

$$=1.00\times10^{19}\frac{m_c^{1/2}m_v^{3/2}m}{m^{*3}}\frac{E_g+\Delta}{E_g+\frac{2}{3}\Delta}NEE_g\kappa^3; \quad (15)$$

κ is the static dielectric constant. The numerical value for C in (15) gives the spontaneous and stimulated functions in units of photons per cm^3-meV-sec when the energies inside the integrals in (14a) and (14b) are in meV. We have ignored the factor $(1+a^{*2}k_b^2)^{-4}$ in Eq. (12), since it greatly reduces the simplicity which results when the matrix element is a constant. The error involved is comparable to other uncertainties in the calculation. Dumke[23] finds the average value of

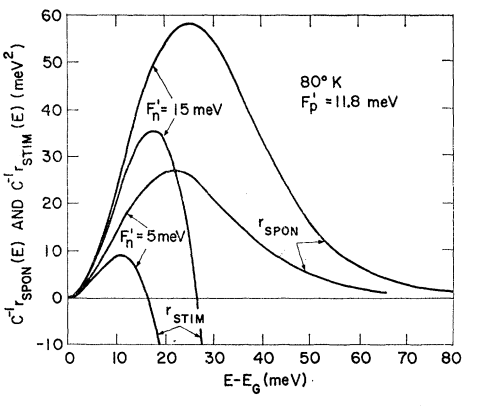

FIG. 1. Spontaneous and stimulated spectral functions at 80°K for parabolic bands, with a hole quasi-Fermi level 11.8 meV within the valence band and electron quasi-Fermi levels 5 and 15 meV within the conduction band. The spontaneous line shape is given by r_{spon} and the gain per unit length is proportional to r_{stim}. The conversion factor C is given in Eqs. (15) and (16b) for GaAs. The calculated curves shown in all the figures are based on the no-selection rule case, Eq. (6).

[24] P. A. Wolff, Phys. Rev. **126**, 405 (1962).

[25] See, for example, E. O. Kane, Phys. Rev. **131**, 79 and 1532 (1963).

[26] An extreme case of a deep impurity level was considered by V. L. Bonch-Bruevich, Fiz. Tver. Tela **4**, 298 (1962) [translation: Soviet Phys.—Solid State **4**, 215 (1962)].

[27] E. O. Kane, Phys. Chem. Solids **1**, 249 (1957).

$(1+a^{*2}k_b^2)^{-4}$ for GaAs to be 0.87 at 77°K and 0.63 at 300°K. Our neglect of this factor therefore tends to overestimate the total transition rate for a given degree of excitation.

Some typical results of the numerical evaluation of $C^{-1}r_{\text{spon}}$ and $C^{-1}r_{\text{stim}}$ are given in Fig. 1, which shows these functions at 80°K for $F'_p=11.8$ meV, and for $F'_n=5$ and 15 meV. A number of the general features of all our results are shown by these curves. As one might expect, the magnitude of both functions increases as the excitation of the system, here represented by F'_n, increases. Because of the general relation between r_{stim} and r_{spon} given in Eq. (8), the peak of r_{stim} occurs at a lower energy than does the peak of r_{spon}, and is smaller in magnitude. Furthermore, r_{stim} vanishes when $E-E_g=F'_n+F'_p$, which corresponds to the condition $E=\Delta F$ given by (8).[28,29] At higher energies r_{stim} becomes negative, corresponding to absorption. In a narrow p-n junction we may assume that $\Delta F=E_g+F'_n+F'_p$ is the electronic charge times the potential difference across the junction, a positive value of ΔF corresponding to forward bias, i.e., to applying a positive voltage to the p-type side of the junction.

We find from (14) and (9) that our model gives $\alpha(E)\sim(E-E_g)^2$ for a nondegenerate system, as one expects for parabolic bands with no selection rule.[30,31] But our assumption of a constant matrix element, with no **k**-selection rule, becomes less valid as $E-E_g$ is increased beyond the activation energy of the impurities, and the absorption will gradually turn over into the $(E-E_g)^{1/2}$ dependence obtained with a **k**-selection rule. We do not expect exciton effects to modify these dependences at the rather high impurity concentrations present in typical cases.[32,33]

The energy gap E_g which enters in our results is the effective energy gap for the material being studied, which, for p-type samples of some semiconductors, may be substantially smaller than the energy gap for pure material. At high doping levels the parabolic approximation will fail, because of the tail in the density of states produced by the random distribution of impurities. This case is briefly considered in Sec. VII.

The effect of varying temperature on the spontaneous and stimulated functions is shown in Fig. 2. We have plotted a series of curves in which $F'_p(T)$ is chosen to keep the hole population constant, with $F'_p=15$ meV when $T=0$°K, while F'_n is varied in such a way that the peak value of $C^{-1}r_{\text{stim}}(E)$ is approximately constant. We see that the amount of excitation needed to maintain a fixed gain increases markedly as the temperature

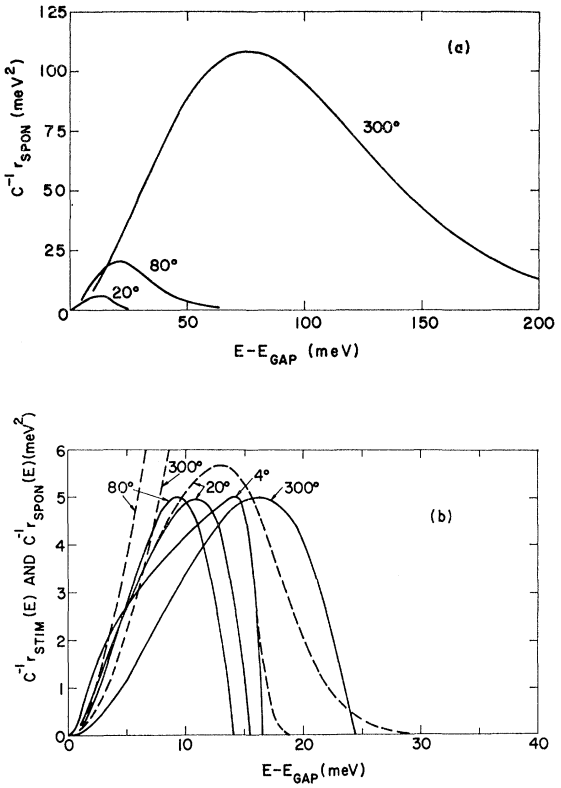

FIG. 2. Spontaneous and stimulated functions at a series of temperatures. The hole quasi-Fermi levels are chosen to keep the hole concentration constant, and the electron quasi-Fermi levels are chosen to keep the peak value of $C^{-1}r_{\text{stim}}$, which is proportional to the gain in the active region, equal to approximately 5 meV^2. According to the constant C' of Eq. (17) this corresponds to a gain of 120 cm^{-1} in GaAs. Fig. 2(a) shows $C^{-1}r_{\text{spon}}$ for 300, 80, and 20°K, and Fig. 2(b) shows $C^{-1}r_{\text{spon}}$ for 20 and 4°K (dashed curves) and the four curves of $C^{-1}r_{\text{stim}}$. The parameters for the curves are: at 4°K, $F'_p=15.0$ meV, $F'_n=1.58$ meV; at 20°K, $F'_p=14.8$ meV, $F'_n=0.6$ meV; at 80°K, $F'_p=11.8$ meV, $F'_n=2.2$ meV; at 300°K, $F'_p=-25.6$ meV, $F'_n=50$ meV.

increases. We shall return to this point in Sec. VI. The spontaneous emission shown for 300°K in Fig. 2(a) probably exceeds the limits of validity of our constant-matrix-element assumption since some of the emission occurs at photon energies which exceed the energy gap by much more than the ionization energy of an acceptor atom. However, the stimulated function is positive only in a limited range of energies from the energy gap, where our approximation is expected to be valid.

[*Note added in proof.* T. N. Morgan has pointed out to us that the typical wave vector change produced by scattering from a screened impurity is of the order of the reciprocal of the screening length. If multiple scattering processes are neglected, this leads to deviations from our no-selection-rule model at energies below the acceptor ionization energy when the acceptor concentration is less than about 10^{19} cm^{-3} in GaAs.]

The results for parabolic bands shown in Figs. 1 and 2, and in later figures, are calculated for specific choices of quasi-Fermi levels and temperature. It is easy

[28] M. G. A. Bernard and G. Duraffourg, Physica Status Solidi **1**, 699 (1961).
[29] R. W. Keyes, Proc. Inst. Elec. Electron. Engr. **51**, 602 (1963).
[30] R. A. Smith, *Semiconductors* (Cambridge University Press, Cambridge, 1961), p. 204.
[31] J. I. Pankove and P. Aigrain, Phys. Rev. **126**, 956 (1962).
[32] R. J. Elliott, Phys. Rev. **108**, 1384 (1957).
[33] R. C. Casella, J. Appl. Phys. **34**, 1703 (1963). We are indebted to Dr. Casella for a preprint of this work.

to see from Eq. (14), however, that a simple scaling will allow the results to be extended somewhat. If we multiply the temperature and all energies by a scaling factor χ, then r_{spon} and r_{stim} will be multiplied by χ^2, and $\mathcal{R}_{\text{spon}}$ will be multiplied by χ^3.

IV. APPLICATION TO GALLIUM ARSENIDE DIODES

To compare the theory with observations on gallium arsenide diodes we assume a uniform density of electrons injected into a uniformly doped p-type material. (This choice is supported by the similarity of the diode emission to the photoluminescence of homogeneous p-type material,[34,35] by the greater efficiency of band-edge photoluminescence in p-type than in n-type GaAs,[36] and by direct photographic observation.[37]) If the electron density is small compared with the equilibrium hole density, the latter will not vary appreciably. We take the density of states of both bands to vary with the square root of the energy to avoid the introduction of more parameters.

Although the hydrogenic model is not strictly applicable to the degenerate valence band, we let the mass m^* which enters the Eq. (15) be that mass which gives the observed ionization energy of acceptor centers when substituted in the hydrogenic formula $E_a = m^* e^4/2\kappa^2\hbar^2$. We shall consider the case of zinc acceptors, and estimate the activation energy to be 34 ± 7 meV from the energy difference between the photoluminescence peak at 1.487 ± 0.005 eV seen in lightly doped p-type GaAs[38] and the optical energy gap, 1.521 ± 0.005 eV,[39] both at liquid-helium temperature. Thus, we estimate that $m^* = 0.39m$, using $\kappa = 12.5$.[40] We shall rather arbitrarily use a density-of-states hole mass $m_v = 0.5m$ in our calculation.

The remaining parameters are better known. We use $m_c = 0.072m$,[41] $E = 1.47$ eV,[10] $\Delta = 0.33$ eV,[42] and $N = 3.6$.[43] Thus, we find for GaAs

$$B = 0.75\times10^{-9}\ \text{cm}^3/\text{sec}, \tag{16a}$$

$$C = 2.6\times10^{23}\ \text{cm}^{-3}\ \text{sec}^{-1}\ \text{meV}^{-3}. \tag{16b}$$

These quantities may well be in error by a factor 2 or more, because of the uncertainties in the parameters and because of the doubtful validity of the hydrogenic model for acceptors.

We define a new constant C', which gives the ratio between $-\alpha$ and the integral in (14b), which is shown in Figs. 1 and 2. With the constants already given we find that

$$C' = \frac{128}{3\pi}\frac{\hbar}{me^4c}\frac{mm_c^{1/2}m_v^{3/2}}{m^{*3}}\frac{E_g}{E}\frac{\kappa^3}{N}\frac{E_g+\Delta}{E_g+\frac{2}{3}\Delta}. \tag{17}$$
$$= 24\ \text{cm}^{-1}\ \text{meV}^{-2}.$$

We can illustrate the use of these constants by applying them to the curves of Fig. 1. At 80°K, a hole quasi-Fermi level of 11.8 meV implies a hole concentration of 3.0×10^{18} cm^{-3}, and the electron quasi-Fermi levels 5 and 15 meV give electron concentrations of 8.7×10^{16} and 2.1×10^{17} cm^{-3}, respectively. The stimulated emission peaks in these curves correspond to absorption coefficients of -220 and -850 cm^{-1}, respectively, and to total spontaneous recombination rates $\mathcal{R}_{\text{spon}} = Bnp$ of 1.9×10^{26} and 4.6×10^{26} cm^{-3} sec^{-1}, respectively.

V. LINE SHAPE FOR VARIOUS STRUCTURES

For the time rate of change of the number of quanta in a single mode of the radiation field within a diode we can write

$$d\mathfrak{N}/dt = -\mathfrak{N}/\tau_{\text{mode}} + [r_{\text{spon}}(E) + \mathfrak{N} r_{\text{stim}}(E)]/\phi(E), \tag{18}$$

where $\mathfrak{N}/\tau_{\text{mode}}$ gives the rate at which photons are lost from the mode because of absorption, transmission out of the sample, or scattering and $\phi(E)$ is the number of modes per unit volume per unit energy interval. In the steady state $d\mathfrak{N}/dt = 0$, and we find

$$\mathfrak{N}(E) = r_{\text{spon}}(E)/[Q^{-1}\omega\phi(E) - r_{\text{stim}}(E)], \tag{19}$$

where we have introduced the quality factor $Q = \omega\tau_{\text{mode}} = E\tau_{\text{mode}}/\hbar$. If we substitute this expression in Eq. (1), we find that the total radiation rate summed over all modes per unit volume and unit energy interval is[44]

$$r(E) = \textstyle\sum_i Q_i^{-1}\omega r_{\text{spon}}(E)/[Q_i^{-1}\omega\phi(E) - r_{\text{stim}}(E)]. \tag{20}$$

The model which leads to Eq. (20) is especially appropriate for describing the line shape of the radiation emitted by nondirectional lasers,[36,45] structures with all four faces made flat and perpendicular to the junction plane, usually by cleaving. In these structures, it is possible to have internally reflected modes with very high Q. If a small fraction of the modes has a Q much higher than the remainder, then the denominator of Eq. (20) will tend to zero for these modes at a value of r_{stim} which is still small compared to $\omega\phi Q^{-1}$ for the low-Q modes. This results in the abrupt appearance of

[34] M. I. Nathan and G. Burns, Appl. Phys. Letters **1**, 89 (1962).
[35] M. I. Nathan, Bull. Am. Phys. Soc. **8**, 201 (1963), and Solid State Electron. (to be published).
[36] M. I. Nathan and G. Burns, in Proceedings of the Third International Symposium on Quantum Electronics, 1962 (to be published).
[37] A. E. Michel, E. J. Walker, and M. I. Nathan, IBM J. Res. Develop. **7**, 70 (1963).
[38] M. I. Nathan and G. Burns (private communication).
[39] M. D. Sturge, Phys. Rev. **127**, 768 (1962).
[40] K. G. Hambleton, C. Hilsum, and B. R. Holeman, Proc. Phys. Soc. (London) **77**, 1147 (1961).
[41] H. Ehrenreich, Phys. Rev. **120**, 1951 (1961).
[42] R. Braustein, Phys. Chem. Solids **8**, 280 (1959).
[43] D. T. F. Marple (unpublished). Reported in the talk by J. D. Kingsley and G. E. Fenner, Bull. Am. Phys. Soc. **8**, 87 (1963).
[44] See also W. G. Wagner and G. Birnbaum, J. Appl. Phys. **32**, 1185 (1961).
[45] F. H. Dill, Jr., 1963 International Solid State Circuits Conference, Philadelphia, February 1963 (unpublished).

a peak in the total emission $r(E)$ near the peak of $r_{\text{stim}}(E)$ as the current increases. This behavior is illustrated by Fig. 3, in which we assume that 1/250th of the modes have a much bigger Q than the remaining modes. The rapid appearance of the peak is well borne out by the experimental results for the nondirectional structures.[46] The threshold for the existence of a substantial amount of stimulated emission, and for line narrowing, is essentially given by the requirement that the smallest denominator in Eq. (20) vanish.

As $r_{\text{stim}}(E)$ approaches $Q_i^{-1}\omega\phi(E)$ for the highest Q modes, the total emission rate, Eq. (20), becomes infinite. Thus, $Q_{\max}^{-1}\omega\phi(E)$ is an upper limit for $r_{\text{stim}}(E)$ for steady-state conditions. This gives an upper limit for the steady-state value of ΔF in the active region in our model. The spontaneous emission rate, $r_{\text{spon}}(E)$, will saturate, and any subsequent increase in the total emission rate will be stimulated emission in the highest Q mode or modes.

The more common structure used for injection lasers is the Fabry-Perot structure, in which two faces of the crystal are accurately flat, parallel to each other, and perpendicular to the junction plane, while the other two faces have been roughened or tilted. We can write the threshold condition for the Fabry-Perot case in the form[47]

$$-\alpha_{\text{active}}(E)=\alpha'+L^{-1}T_n, \tag{21}$$

where $-\alpha_{\text{active}}(E)$ is the gain per unit length in the active region, related to $r_{\text{stim}}(E)$ by Eq. (9), and α' is an effective loss term. This is an approximate form of the threshold condition

$$-\alpha_{\text{active}}(E)=\alpha'+L^{-1}\ln(R_n^{-1}), \tag{22}$$

where R_n is the reflectivity of the ends, which can be deduced from the requirement that the amplitude of the wave be unchanged after a complete traversal back and forth through the sample. The two expressions are equivalent if $1-R_n=T_n\ll 1$.

VI. TEMPERATURE DEPENDENCE OF LASING THRESHOLD

An important consequence of the model we have proposed is its prediction of the temperature dependence of the current at which lasing occurs. The condition for threshold for a Fabry-Perot structure is given in Eq. (22), and the corresponding condition for a nondirectional laser is similar, since in both cases the gain in the active region, measured by the peak value of $-\alpha(E)$, must be great enough to overcome losses within the crystal and the loss due to transmission across the surface. The transmission losses will not change significantly with temperature, but the other losses, represented by α' in (22), may well vary with temperature.

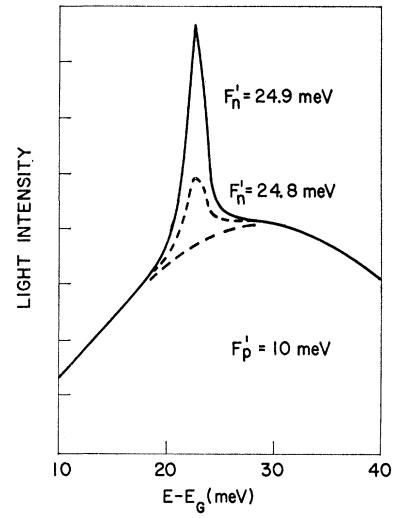

FIG. 3. Spectrum of the total radiation emitted by a diode in which a small fraction of the modes has a much higher Q than the remaining modes.

We may think of the loss term α' as arising from the absorption of light which penetrates into the inactive region, together with free-carrier absorption and possible scattering effects within the active region itself. Free-carrier absorption does increase with increasing temperature in both n-type[48] and p-type[49] GaAs, and the penetration of the light into the inactive region may also lead to increased loss at higher temperatures.

Since the loss term α' is hard to estimate quantitatively, and since there is evidence that in some Fabry-Perot diodes the major loss term is the surface loss,[38] we shall assume that the threshold condition is that the maximum value of $-\alpha(E)$ be independent of temperature. The physical cause of the temperature dependence of threshold is therefore taken to be the decrease in the degeneracy of the electron and hole population as the temperature is increased. At higher temperatures the carrier populations are distributed over larger energy ranges giving larger amounts of spontaneous emission, and therefore a higher current, for the same degree of population inversion.

To estimate the current, we note from Eq. (20) that the total recombination rate somewhat below threshold is only slightly greater than the spontaneous recombination rate, if the fraction of high-Q modes is small. (Only in this case can we speak of a well-defined threshold.) If the active region is of thickness d and if a fraction η'' of the current carriers crossing the junction recombine via the radiation band which leads to the lasing mode, then we have, using (6d),

$$J/e=d\mathcal{R}_{\text{spon}}/\eta''=Bnpd/\eta''. \tag{23}$$

In Fig. 4 we give a series of curves at various temperatures for $C^{-1}r_{\text{stim}}(\max)$ versus $C^{-1}\mathcal{R}_{\text{spon}}$. The curves were calculated, using the model described in Secs. III

[46] G. Burns and M. I. Nathan, Proc. Inst. Elec. Electron. Engrs. **51**, 471 (1963). See also Ref. 36.
[47] G. J. Lasher, IBM J. Res. Develop. **7**, 58 (1963).
[48] W. G. Spitzer and J. M. Whelan, Phys. Rev. **114**, 59 (1959).
[49] W. J. Turner and W. E. Reese, Bull. Am. Phys. Soc. **8**, 311 (1963), and J. Appl. Phys. (to be published).

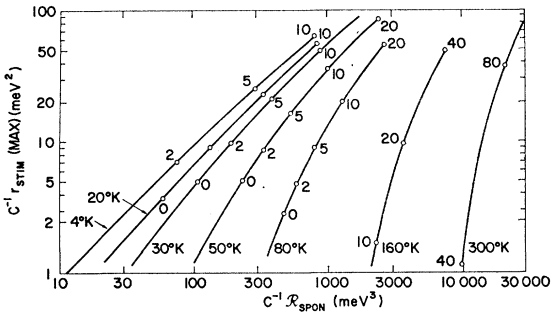

FIG. 4. Curves of $C^{-1}r_{\text{stim}}(\max)$ as functions of $C^{-1}\mathcal{R}_{\text{spon}}$ for a series of temperatures. The peak bulk gain, in cm^{-1}, can be obtained for GaAs by multiplying the ordinate by the factor C' in Eq. (17), and the current density can be obtained by multiplying the abscissa by the factor given in Eq. (24). The hole quasi-Fermi level is 14.6 meV at 30°K, 13.8 meV at 50°K, 1.8 meV at 160°K, and has the values given in Fig. 2 at the remaining temperatures. The electron quasi-Fermi levels, in meV, corresponding to the circled points are marked on the figure.

and IV, with a fixed hole concentration corresponding to $F'_p=15$ meV at 0°K, or to 3×10^{18} cm^{-3} for the heavy-hole mass $m_v=0.5m$ assumed for GaAs in Sec. IV. They show how the gain, measured by the ordinate, depends on the current, which is proportional to the abscissa.

The temperature dependence of the threshold current for lasing is easily deduced from Fig. 4 by plotting the value of $C^{-1}\mathcal{R}_{\text{spon}}$ required to give a fixed value of $C^{-1}r_{\text{stim}}(\max)$. The results are shown in Fig. 5, where the values of $C^{-1}r_{\text{stim}}(\max)$ are shown with the individual curves. The insets in Fig. 5 show schematically the position of the laser spike relative to the peak of the spontaneous emission for the gain points marked A and B, at 80°K, and show that the spike occurs closer to the spontaneous peak at higher gains.

The conversion factor for the gain is the constant C' given in Eq. (17). Thus, for the numbers given in Sec. IV for GaAs, we find the gain in the active region, in cm^{-1}, by multiplying the ordinate of Fig. 4, and the parameters labeling the curves of Fig. 5, by 24. The factor with which we must multiply $C^{-1}\mathcal{R}_{\text{spon}}$ to obtain the current density in A/cm^2, as given by Eq. (23), is

$$Ced/\eta''=4.2d/\eta'', \tag{24}$$

where d is the thickness of the active region in microns, if we take the value of C from (16b).

The curves in Fig. 5 show the threshold current density J_{th} to vary approximately as the 1.8 to 2.6 power of the absolute temperature, depending on the gain required at threshold, and to level off at lower temperature. If we use the position of the lasing spike at 77°K in nondirectional lasers as a criterion for deciding which gain curve to use, we would pick a curve roughly halfway between the curves marked A and B in Fig. 5, for which $J_{\text{th}}\sim T^{2.2}$. If we consider that the loss term α' in Eq. (22) is increasing with temperature, so that the required gain at threshold is higher at 300°K than at 77°K, we find that the calculated temperature dependence agrees fairly well with the experimental result[50] $J_{\text{th}}\sim T^3$. The experimental curves also tend to flatten at low temperature as shown in Fig. 5.

The curves of Fig. 5 suggest that if the threshold of a unit can be reduced, say by improving the reflectivity or the quality of the ends of a Fabry-Perot diode, the ratio $J_{\text{th}}(77°\text{K})/J_{\text{th}}(4°\text{K})$ should increase. Conversely, if the surface quality deteriorates, the threshold ratio should decrease. This conclusion is qualitatively supported by a comparison of threshold currents before and after silvering on a number of Fabry-Perot diodes.[51]

If we had attempted to determine the temperature dependence of the threshold current from the zero-gain condition $\Delta F=E_g$, or, equivalently, $F'_n+F'_p=0$, retaining the condition that the hole concentration remains constant as the temperature changes, we would have found a temperature dependence steeper than that shown in Fig. 5 and also steeper than the experimental result.

The results of Figs. 4 and 5 show that at room temperature a rather large concentration of minority carriers must be injected to reach threshold even for relatively low gain. Thus, taking the parameters assumed for GaAs in Sec. IV, we find that even the lowest gain in Fig. 5 requires an injected electron concentration of 1.2×10^{18} cm^{-3} at 300°K. These results suggest that it may be easier to reach threshold at room temperature in units with a more heavily doped p-type active region.

The temperature dependence of the threshold current density in GaAs injection lasers may be understood qualitatively as the result of the increased minority

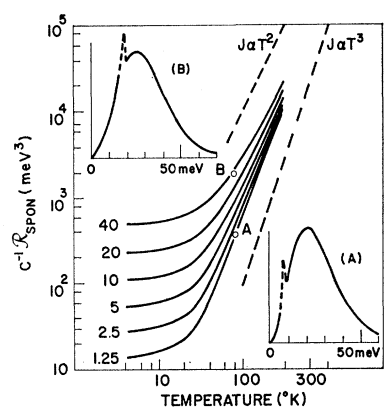

FIG. 5. Temperature dependence of the threshold current density. The parameter labeling the curves is the value of $C^{-1}r_{\text{stim}}(\max)$, which is proportional to the gain in the active material. These values are obtained from Fig. 4, and the same conversion factors apply. The two insets show schematically the line shape and position of the lasing spike, as in Fig. 3, corresponding to the points marked A and B.

[50] G. Burns, F. H. Dill, Jr., and M. I. Nathan, Proc. Inst. Elec. Electron. Engrs. 51, 947 (1963).
[51] M. I. Nathan and G. Burns (private communication).

TABLE I. Comparison of theoretical and experimental results for two silvered Fabry-Perot diodes made from a zinc diffusion into a substrate containing 9×10^{17} electrons per cm^3. The first row gives the full width of the spontaneous emission at half-maximum, and the second row gives the energy by which the lasing spike lies below the peak of the spontaneous emission. J_{th} is the threshold current density and F'_p and F'_n are the hole and electron quasi-Fermi levels relative to the respective band edges. The values of F'_n were chosen to yield the factor 13 for $J_{th}(77°K)/J_{th}(4.2°K)$ and to give the same gain at both temperatures.

	77°K		4.2°K	
	Experiment[a]	Theory	Experiment[a]	Theory
Linewidth [meV]	23.5/23.5	27.4	13.9/14.5	11.8
Spike shift [meV]	6.6/6.3	11.8	−2.5/0.0	0.1
$J_{th}(77°K)/J_{th}(4.2°K)$	13.4/12.7	13.0		
$J_{th}(77°K)$[A/cm^2]	940/1280	$1870d[\mu]/\eta''$		
F'_p [meV]		12.1		15.0
F'_n [meV]		0.1		1.1

[a] We are indebted to G. Burns and M. I. Nathan for permission to use the unpublished experimental values.

carrier population which is required to produce a given gain at higher temperatures, when the carriers are distributed over a much wider range of states.

In the limit of low temperature, there is a simple relation between the current density and the gain in the active region, given by Eqs. (1) and (2) of Ref. 47. Any calculation of the spectral functions $r_{spon}(E)$ and $r_{stim}(E)$ may be used to generalize this relation to apply at all temperatures. Thus, we may use Eqs. (9) and (23) to express the current density required to reach a gain $-\alpha$ in the active region as

$$J=8\pi\gamma eN^2d\Delta E(-\alpha)/h\lambda^2\eta'', \tag{25a}$$

where ΔE is the full width of the spontaneous emission at half-maximum, h is Planck's constant, λ is the wavelength of the radiation in vacuum, and

$$\gamma=\mathcal{R}_{spon}/\Delta E r_{stim}(\max) \tag{25b}$$

is a dimensionless factor introduced to account for line shape and temperature effects. We note that γ does not depend on the value of the conversion factor C of Eq. (15). The numerical expression for (25a) is

$$J[\mathrm{A/cm^2}]=0.0974N^2\gamma d\Delta E(-\alpha)/\lambda^2\eta'', \tag{25c}$$

where d and λ are measured in microns, α in cm^{-1}, and ΔE in meV. For GaAs this gives

$$J[\mathrm{A/cm^2}]=0.18\gamma d\Delta E(-\alpha)/\eta''. \tag{26}$$

The factor γ, as computed from the parabolic band model that led to Fig. 4, is plotted in Fig. 6 as a function of $C^{-1}r_{stim}(\max)$, with the upper scale giving the conversion to the gain in the active region for GaAs. This conversion is only approximate, since it depends on the parameters estimated in Sec. IV; an error in these parameters will require a horizontal shift of the upper scale.

A quantitative comparison of our results with experiment is given in Table I for two silvered Fabry-Perot units chosen because the lasing spike approaches the peak of the spontaneous emission as the temperature is lowered, and because the spontaneous emission peak does not have a large energy shift with current at low temperature. The hole quasi-Fermi level was picked to give a linewidth somewhat smaller than the observed width at 4.2°K, since a tail in the density of states in the conduction and valence band will tend to increase the experimentally observed width over the width found with our parabolic model, and will tend to give a somewhat more symmetrical line, in better agreement with experiment. Another broadening factor present in real diodes but not in our model is the nonuniformity of the degree of excitation as the distance from the junction varies. The electron quasi-Fermi level is chosen to give the observed factor of 13 between threshold current densities at 77° and 4.2°K.

In Table I we compare the calculated and observed values of the linewidth of the spontaneous emission near threshold and of the position of the lasing spike relative to the spontaneous emission peak at 77 and 4°K. The agreement is satisfactory in view of the many simplifications that have been made in our model. If we use the

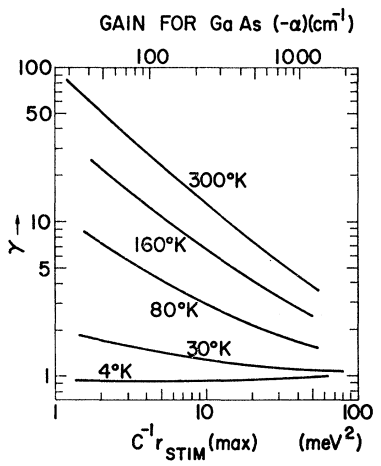

FIG. 6. Finite temperature correction to the threshold relation. When the quantity γ is inserted in the threshold relation, Eq. (25), one obtains the threshold current density in terms of the thickness of the active region, the observed spontaneous linewidth, and the threshold gain. The 4°K curve is essentially a zero-temperature curve; its deviation from unity is caused by small shape-dependent factors.

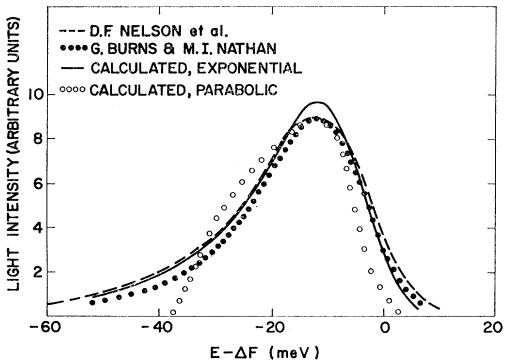

FIG. 7. Calculated and experimental spontaneous line shapes at 20°K. The experimental curves are those of Nelson *et al.*, Ref. 53, and of Burns and Nathan (to be published), for diodes whose peak wavelength varies rapidly with current. The solid curve has been calculated for a conduction band density of states proportional to $\exp(E/E_0)$, with $E_0=15$ meV, and a parabolic valence band with $F'_p=14.8$ meV. The open circles were calculated for parabolic conduction and valence bands, taking $F'_n=1$ meV, and $F'_p=29.9$ meV, the latter value having been chosen to approximate the halfwidth of the experimental curves.

value of J_{th} at 77°K, together with the quasi-Fermi levels that gave the calculated results in Table I, we find that $d/\eta''=0.6\,\mu$, a value that must be considered uncertain to at least a factor of 2. Other Fabry-Perot units have given values of d/η'' of several microns if $-\alpha$ in Eq. (26) is equated to the end loss.

A crude estimate of the dimensions of the active region can be made if we assume that at 77°K the diffusion constant of electrons in the p region is $D\approx 10$ cm²/sec, and that the hole concentration in the active region is $\approx 3\times 10^{18}$ cm^{-3}. Then from Eqs. (11) and (16a) we deduce that $\tau\approx 0.4_4\times 10^{-9}$ sec, so that a characteristic distance for the decay of the injected electrons is $(D\tau)^{1/2}\approx 0.7\,\mu$. The result is only approximate, because the acceptor concentration is varying rapidly near the junction in the typical Zn-diffused GaAs diode, but it is in good qualitative agreement with the thicknesses deduced from the experimental results, as given in the previous paragraph.

VII. EFFECTS OF A CONDUCTION BAND TAIL

At low temperatures and low current densities our parabolic approximation fails, since the occupied states in the conduction band will then lie in the band tail associated with the randomness of the impurity distribution. Under these conditions, the peak of the spontaneous emission is observed to depend rather strongly on the current through the unit.[52–54]

Our general procedure is quite simply applied even when one or both bands are nonparabolic, provided we can continue to assume that the matrix element is independent of the initial and final states. Then we can use Eq. (6), substituting the appropriate densities of states. As a numerical illustration we have taken $T=20$°K and compared a parabolic conduction band with $F'_p=29.9$ meV and $F'_n=1$ meV with an exponential conduction band whose density of states is proportional to $\exp(E/E_0)$, with $E_0=15$ meV, and $F'_p=14.8$ meV. The results are shown in Fig. 7, along with experimental line shapes found by Nelson *et al.*[53] and by Burns and Nathan.[55] The large value of F'_p for the parabolic case was chosen to fit the experimentally observed width.

Comparison of the calculated and experimental results in Fig. 7 shows that a line based on a parabolic band agrees quite poorly with the observed shape, while a line based on an exponential conduction band tail agrees quite well. The agreement is partly fortuitious, since other factors which would broaden the line, such as the contribution of other parts of the p-n junction to the radiation, and the effects of a valence band tail, have been ignored. Thus, we expect that the value $E_0=15$ meV used to calculate the exponential curve in Fig. 7 is an overestimate. Nelson *et al.*[53] fit the shift of the spontaneous emission peak with current for their diode by taking $E_0=8.7$ meV.

In the energy range in which the conduction band is exponential, the shape of the emission line will be independent of the electron quasi-Fermi level (or the current or voltage). The peak of the spontaneous emission will be related to the voltage across the junction by $E_{\text{peak}}=\text{eV}-\text{eV}_0$,[54,56] where $\text{eV}=F_n-F_p$. For the calculated case in Fig. 7, we find $\text{eV}_0=12$ meV. The corresponding values for $E_0=5$ and 10 meV are $\text{eV}_0=7$ and 10 meV, respectively.

As KT approaches E_0 from low temperatures, the spontaneous line should broaden and V_0 becomes negative. Archer *et al.*[56] report $V_0=-14$ meV for a diode having an n doping of 2.5×10^{18} cm^{-3} at $T=77$°K. Our calculation would give this for $F'_p=12.1$ meV and $E_0=8$ meV. In this case the peak shift data gave $E_0=10$ meV. For $KT=E_0$ the number of electrons per unit energy interval becomes independent of energy in the experimental range, resulting in a very broad emission. Such spectra have been seen by Burns and Nathan[55] for more lightly doped diodes at lower temperatures.

APPENDIX. TRANSITIONS INVOLVING DEGENERATE LEVELS OF A DEFECT SITE

The expressions of Sec. II are based on the Fermi-Dirac occupation probability of Eq. (7), which applies when the energy levels of upper and lower states lie in a continuum, and the wave functions of the states are not well localized. On the other hand, if isolated impurity or defect levels are present, several levels of

[52] J. I. Pankove, Phys. Rev. Letters **9**, 283 (1962).
[53] D. F. Nelson, M. Gershenzon, A. Ashkin, L. A. D'Asaro, and J. C. Sarace, Appl. Phys. Letters **2**, 182 (1963).
[54] R. J. Archer and J. C. Sarace, Bull. Am. Phys. Soc. **8**, 310 (1963).
[55] G. Burns and M. I. Nathan (unpublished).
[56] R. J. Archer, R. C. C. Leite, A. Yariv, S. P. S. Porto, and J. M. Whelan, Phys. Rev. Letters **10**, 483 (1963).

the same energy may arise from the presence of a single site. Coulomb interactions between electrons on the same donor site will usually be sufficiently strong that if more than one of the g_u degenerate states associated with the site is occupied, the resulting energy level is far removed from the energy range of interest. Similarly, an acceptor site may give rise to g_l levels for a hole, but no more than one of these can be occupied without a major shift of energy.

The condition that no more than one of the g_u levels associated with a donor site be occupied leads to an occupation probability[57]

$$f_u = \{g_u + \exp[(E_u - F_n)/KT]\}^{-1}. \qquad \text{(A1)}$$

For the lower states, it is convenient to let f_l' denote the probability that one of the g_l levels associated with the acceptor site be occupied by a hole. Then we find

$$f_l' = \{g_l + \exp[(F_p - E_l)/KT]\}^{-1}. \qquad \text{(A2)}$$

If individual states are independent, we have $g=1$, and the results reduce to those of Eq. (7).

The downward transition between a particular one of the g_u upper states and one of the g_l lower states will take place only if there is an electron in the upper state and a hole in the lower state. We have, therefore,

$$r_{\text{spon}} \approx f_u f_l', \qquad \text{(A3)}$$

where all the factors in Eq. (3a) that do not depend on the occupations of the levels have been omitted.

[57] See p. 87 of Ref. 30.

The stimulated function contains both downward and upward transitions. The former contribution will be proportional to $f_u f_l'$ as in (A3). On the other hand, an upward transition of the same energy can take place only if none of the g_l lower levels is occupied by a hole and none of the g_u upper levels is occupied by an electron. The probability that there is no hole on any of the lower levels is $1-g_l f_l'$, and the probability that there is no electron on any of the upper levels is $1-g_u f_u$. Thus, the stimulated function will be

$$r_{\text{stim}} \approx [f_u f_l' - (1-g_l f_l')(1-g_u f_u)]. \qquad \text{(A4)}$$

It may well happen that selection rules forbid some of the $g_u g_l$ possible transitions, or that some of the matrix elements have different values from others. But these possibilities affect r_{spon} and r_{stim} in the same way, and we find, from Eqs. (A1)–(A4)

$$r_{\text{stim}}(E) = r_{\text{spon}}(E)\{1-\exp[(E-\Delta F)/KT]\}, \qquad \text{(A5)}$$

just as in Eq. (8).

ACKNOWLEDGMENTS

We are indebted to G. Burns and M. I. Nathan for many discussions of experimental results, and to W. P. Dumke for discussions concerning the radiative recombination mechanism. We also thank H. Cheng, R. W. Keyes, T. N. Morgan, and K. Weiser for helpful comments on the manuscript.